-RESEARCH PAPER-

International Journal of Mining and Geo-Engineering

IJMGE

IJMGE 58-3 (2024) 271-279

DOI: 10.22059/IJMGE.2024.369526.595129

Slope stability analysis of the open-pit walls using artificial intelligence

Vahid Amini [a] , Sayed Hassen Khoshrou [a, *] , Zohre Iranmanesh [a]

[a] *Amir Kabir University of Technology, Tehran, Iran.*

Article History:

Received: 12 December 2023.

Revised: 13 February 2024.

Accepted: 8 April 2024.

ABSTRACT

Slope stability analysis is widely recognized as a crucial aspect in rock mechanics engineering, playing a fundamental role in the design of various rock and soil structures like mining slopes, roads, and tunnels. Over time, several methods have been proposed to address stability concerns, including limit equilibrium methods, numerical approaches, and artificial intelligence techniques. In this study, we conducted stability analysis of mine wall slopes using a neuro-fuzzy integrated approach (ANFIS). Using data from the Choghart iron mine, we developed two neuro-fuzzy networks to analyze the safety and stability of circular failures under static loading conditions. Six parameters were identified as the most significant inputs in the circular failure model, with safety factor (SF) and stability (S) state as outputs, analyzed under two different scenarios. The results obtained indicate that the stability and safety analysis networks exhibit low error and high correlation, with an average error for the safety factor and stability of 0.05 and 0.013, respectively, demonstrating the network's high generalization capability. Additionally, the artificial intelligence outputs of test data identified the southern wall of the mine as the most critical section, calculating the safety factor and stability of this area to be 0.81 and 0.66, respectively.

Keywords: *Slope stability, Safety factor, Artificial intelligence..*

1. Introduction

Open-pit mining is a notably economical approach in mining, facilitating the utilization of maximum equipment capacity, enhanced extraction rates, and lower-grade minerals. Determining the pit wall slopes represents a crucial design parameter in open-pit mining. If the wall slope is considered too shallow, the amount of waste extraction increases significantly. On the other hand, selecting steeper wall slopes reduces safety and increases the likelihood of collapse. Consequently, choosing an optimal slope to prevent excessive waste extraction and reduce the risk of wall failure is essential. Slopes can be classified into two categories based on the type of failure that may occur: translation and rotation. Failure in high-strength rocks typically starts as translation and in low-strength rocks as rotation, which can subsequently continue in various forms. Slope failure is also known as slide and landslide, which can occur gradually.

Based on conducted studies, numerous factors influence the stability of both natural and artificial slopes, including the geometry of the failure plane, the homogeneity or heterogeneity of soil layers, tensile cracks, seismic or dynamic loads, and water pressure. Various methods have been proposed to address slope stability, including conventional (limit equilibrium) methods, numerical methods, and artificial intelligence techniques. Conventional methods widely used in stability analysis include the Fellenius Method, Bishop Method, Janbu Method, Spencer Method, and Morgenstern-Price Method, all sharing common characteristics and limitations. Among these methods, those considering lateral forces between segments, such as the Janbu Method, can lead to numerical instability of the problem under certain conditions. When numerical instability occurs, the selected method may struggle with convergence or yield inappropriate results. Methods accounting for the sum of forces across all segments can render manual safety factor calculations laborious, time-intensive, and repetitive. With the advent of various computer codes based on limit equilibrium methods, this calculation process has been greatly simplified and expedited. In all approaches except for the Fellenius Method, the safety factor is defined as the ratio of the actual shear resistance at a point to the shear resistance at that point, and it is assumed to remain constant along the entire slip surface [1].

Numerical methods play a crucial role in analyzing slope stability, with both the finite element and finite difference methods serving as solutions for nonlinear issues. While these numerical methods are more complex compared to conventional techniques, they provide a comprehensive understanding of slope deformation and collapse. The insights offered by these methods, including details on the safety factor and the slip surface, offer substantial advantages when combined with results from traditional methods.

Moreover, considering the uncertainties involved in this matter, such as those arising from the inherent characteristics of slope materials, the time-dependent variability of these properties, and uncertainties linked to inadequate and inappropriate data, along with the impact of various factors and their interactions in slope stability modeling, physical models encounter difficulties in accurately representing actual conditions and accounting for these significant factors. Physical models typically necessitate data on slope geometry and soil characteristics, which are often unavailable. In such situations, artificial intelligence methods can be appropriate and efficient. As these methods rely on laboratory or in-situ data, analyzing the impact of different factors on the safety factor in these models becomes more straightforward. Intelligent networks with learning capabilities, such as smart neural networks and hybrid intelligent systems, can accurately model slopes even in the absence of certain data related to soil characteristics and slope geometry.

* Corresponding author. *E-mail address:* khoshrou@aut.ac.ir (S. H. Khoshrou).

Researchers employ soft computing methods to tackle complex issues characterized by insufficient and uncertain information. These methods encompass a range of computational techniques, including fuzzy algorithms, intelligent neural networks, Support Vector Machine (SVM), evolutionary approaches, machine learning, and probabilistic reasoning. The first neural network model was designed by McCulloch & Pitts, which is recognized as the pioneering study in artificial intelligence. Subsequently, numerous researchers have proposed various methods and algorithms based on this initial artificial neural network model. In 1994, soft computing was formally recognized as a part of computer science, leading to the introduction of a variety of new algorithms, including ANFIS and swarm intelligence.

Reviews of past studies indicate that artificial intelligence methods used to address slope stability issues include fuzzy logic, intelligent neural networks, genetic algorithms, adaptive neuro-fuzzy inference systems, hybrid and metaheuristic algorithms such as bee colony and ant optimization algorithms, and particle swarm optimization. Most models presented utilize the geotechnical properties of slope-forming materials and the filler materials in joints as input parameters. However, some studies, like the model suggested by Chen et al. [2], have considered parameters such as rock type, slope aspect, number of joint sets, joint spacing, and the bedding-slope relationship as inputs. Although the majority of studies predominantly focus on the safety factor, the condition of stability, and the characteristics of the slip surface as outputs, there are exceptions, such as the model proposed by Chen and Zhen [3], where displacement is considered as the output. Typically, these methodologies address both circular and non-circular failure mechanisms in static conditions. However, some researchers have expanded their analysis to dynamic situations, incorporating the impact of horizontal seismic accelerations on slope stability. In this study, the stability and safety factor of mine walls at the Choghart iron mine have been assessed using an adaptive artificial intelligence approach employing data from the mine. The input parameters considered include unit weight, cohesion, internal friction angle, and geometrical slope parameters such as slope height and slope angle, along with external forces, including the ratio of pore water pressure. For the first scenario (ANFIS1), the safety factor was analyzed as the output, while the stability condition was the focus for the second scenario (ANFIS2). It should be mentioned that the desired stability and safety factor level of the mine wall is defined between 0-1 and 0.97-2.05 respectively, the upper banks of the mentioned interval indicate the stability (S) and high safety factor of the mine wall, and the lower bank indicates the instability (IS) and low safety factor. In Table (1), a summary of the researches carried out in this field is given.

Table 1: Summary of research records in slope stability analysis.

Author	Moot Point				Computational Methods *														
	Displacement Rate	Critical Failure Plate	Stability Condition	Safety Factor	ELM	SVM	BC	DENN	ANFIS	EPR	AC	FS	TS	HS	SOM	PSO	SAM	ANN	GA	MLE
Sah et al (1994) [4]				*																*
Goh (1999,2000) [5,6]		*																	*	
McCombie (2002) [7]		*																	*	
Lu (2003) [8]				*														*		
Yang et al (2004) [9]			*	*															*	
Sakellariou (2005) [10]		*																*		
Ferentinou (2007) [11]	*	*													*			*		
Cheng et al (2007) [12]				*							*		*	*		*	*		*	
Park et al (2008) [13]		*										*								
Li et al (2008) [14]		*																	*	
Choobbasti et al (2009) [15]				*															*	
Zhou et al (2009) [16]			*															*		
Chen et al (2009) [2]				*														*		
Shangguan et al (2010) [17]		*																*		
Ahangar et al (2010) [18]			*							*										
Daftaribesheli et al (2011) [19]			*										*							
Chen et al (2011) [20]			*	*					*											
Das et al (2011) [21]				*				*												
Park et al (2012) [22]				*									*							
Erzin et al (2012) [23]		*																*		
Kang et al (2013) [24]			*				*													
Samui (2013) [25]	*					*														
Chen et al (2013) [3]				*														*		
Erzin et al (2013) [26]				*														*		
Manouchehrian et al (2014) [27]				*															*	
Liu et al (2014) [28]				*	*															
Xue et al (2017) [29]			*													*				

* MLE (Maximum Likelihood Estimation of Slope Stability), GA (Genetic Algorithm), ANN (Artificial Neural Network), SAM (Simulated Annealing Method), PSO (Particle Swarm Optimization), SOM (Kohonen Self-Organizing Maps, HS (Harmony Search), TS (Tabu Search), FS (Fuzzy Search), AC (Artificial Bee Colony), EPR (Evolutionary Polynomial Regression), ANFIS (Adaptive Neuro-Fuzzy Inference System), DENN (Differential Evolution Neural Networks), BC (Bee Colony), SVM (Support Vector Machine), ELM (Extreme Learning Machine).

2. Project Introduction

The Choghart iron mine is situated 120 kilometers southeast of the Yazd city, 75 kilometers southwest of the city of Bahaabad, on the fringe of the central desert of Iran. It is characterized by a hot and dry climate with low humidity. Initially, the elevation of the Choghart deposit was approximately 1,286 meters above sea level, standing about 150 meters above the surrounding area. With a geological reserve of 193 million tons and an extractable reserve of 177.2 million tons, this mine is considered one of the largest in the country. Mining operations began in September 1971 and continued until the end of 2011, during which over 131 million tons of iron ore were extracted. Originally operating as a quarry, the mine transitioned to an open-pit operation in 1995, once it reached ground level (elevation 1140). According to the latest proposed plan, the final elevation of the mine is expected to be 820 meters, resulting in a final wall height of 340 meters. Field observations have revealed instability in parts of the mine, with numerous collapses occurring annually. This situation necessitates serious consideration and analysis of wall stability, especially considering the increasing depth of the mine.

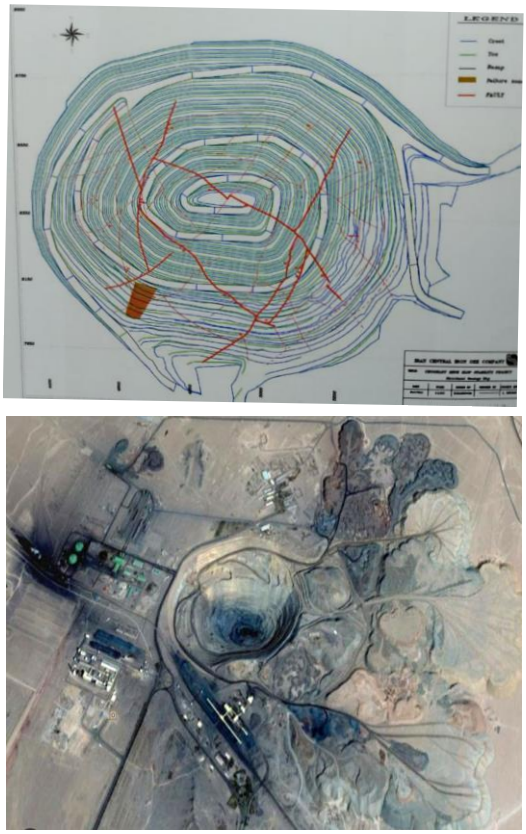

Figure 1. aerial photo and fault map of Choghart iron mine [38].

Due to the limited area of the investigation zone and the homogeneity of rock types, a diverse range of geological structures cannot be observed and analyzed. In other words, the presence of specific lithology restricts the observation of structures to those such as faults, small-scale folding, and joint systems at the outcrop level. Geologically, the structures in this region fall within the mesoscopic scale, considering their scale and the degree of deformation. This includes features such as folds spanning several centimeters, joints, and faults extending over several meters.

3. Materials and Methods

Over the past few decades, soft computing has emerged as an approximate solution methodology for problems requiring precise formulations or addressing indistinct issues, distinguishing it from traditional methods known as classical modeling. It has found particular application in tasks such as decision-making, system modeling, and control. These systems function by modeling the human mind's ability to process information in parallel, adeptly analyzing and learning in situations characterized by uncertainties and imprecise data. Key components of this approach include fuzzy logic, intelligent neural networks, and adaptive neuro-fuzzy inference systems. The term ANFIS was first introduced by Jang in 1993 [30]. In that year, Jang presented a new model based on fuzzy theory, which integrated certain characteristics of neural networks, such as learning and parallelization. This system also harnesses the adaptive properties of neural networks to determine the parameters of the fuzzy system, fuzzy rules, and the type of membership function. For this purpose, network partitioning and clustering methods can be employed. In these networks, fixed and linear outputs can be used to achieve subsequent parameters, where linear functions are known as first-degree Sugeno fuzzy inference systems and fixed functions are recognized as zero-degree [31]. Initially utilized in the field of neuro-fuzzy control, the application of these systems has since expanded and is now used in fields such as control, data analysis, and decision support [32].

ANFIS functions as a fuzzy inference system, operating similarly to a standard fuzzy system [33]. Thus, it requires initial organization. The initial network structure identification involves tasks such as selecting independent input variables, segmenting the input space, deciding the number of membership functions for each input, establishing the number of fuzzy rules, defining the hypothesis part of each rule, determining the consequent part of each fuzzy rule, and setting initial parameters for the membership functions. Typically, there are two methods for deriving fuzzy rules: network partitioning and clustering. In the present study, the emphasis is on the clustering method.

3.1. Fuzzy Clustering

Clustering plays a vital role in modern data mining methods. The fundamental concept of clustering is to partition the initial dataset into homogeneous groups based on their shared characteristics. In classical clustering, each cluster exhibits a distinct pattern, but in practice, some patterns may belong to more than one cluster with varying degrees of membership. This concept is captured through fuzzy clustering as opposed to classical clustering. Fuzzy clustering itself is divided into two types: the Subtractive Clustering Method (SCM) and clustering based on Fuzzy C-Means (FCM).

3.1.1. Fuzzy Clustering Using the Fuzzy C-Means Algorithm

This algorithm aims to minimize the objective function, which represents the distance of each data point from the cluster center. This distance is weighted using the membership degree of the data. In this algorithm, the cluster center shifts among different clusters through successive iterations until the objective function reaches its minimum value. The outcome is a set of clusters that are as dense as possible while maintaining an appropriate distance from each other [34]. Challenges associated with this algorithm include the potential for stopping at a local minimum and sensitivity to initial values such as the number and initial centers of the clusters [35, 36]. There are two general methods for validating clusters. The first method involves running and iterating the algorithm, incrementing the number of clusters from 1 to n-1, and examining the algorithm's characteristics and the partitioning space using specific indices. The second method involves executing an algorithm that calculates the optimal number of clusters itself, such as the Subtractive Clustering Method.

3.1.2. Subtractive Clustering Method

In this method, each data point, rather than grid points, is regarded as a potential cluster center. Using this approach, the effective "grid points" to be examined are simply equal to the number of data points, independent of the dimensions of the problem. A key aspect of this method is its speed, derived from the fact that no form of nonlinear

optimization is repeated in this algorithm. Furthermore, calculations are linearly related to the dimensions of the problem [37]. If a set consisting of n data points in an M-dimensional space is considered, and it is assumed that the data points are normalized in each dimension, the coordinate range in each dimension will be consistent. In this method, each data point is regarded as a potential center, and its potential is calculated as follows:

$$P_i = \sum_{j=1}^{n} e^{-\alpha\|x_i - x_j\|^2} \quad (1)$$

In this Equation:

$$\alpha = \frac{4}{r_a^2} \quad (2)$$

In Equation (2), r_a is a positive constant representing the effective neighborhood radius. According to the equations mentioned, each data point's potential is a function of its distance relative to other points. In this algorithm, a point with many other points in its vicinity has the highest potential, and data points outside the effective radius have the least impact on the potential value [34]. After calculating the potential of each point, the data point with the highest value is identified as the first data center. If x_1 is the location of the first cluster center and p_1 is its potential value, the potential of other points is calculated using the following formula:

$$P_i = p_i - p_1 e^{-\beta\|x_i - x_1\|^2} \quad (3)$$

In this Equation:

$$\beta = \frac{4}{r_b^2} \quad (4)$$

In Equation (4), r_b represents a positive number denoting the effective neighborhood radius. According to Equation (3), the potential value of each data point as a center diminishes. Data points near the center of the first cluster will have the lowest potential and are unlikely to be chosen as the next cluster center. Typically, r_b is set to be 1.5 times larger than r_a to prevent the cluster centers from being too close. Once the potentials of the points are adjusted according to Equation (3), the point with the highest potential is selected as the center of the first cluster. Subsequently, after determining the k-th cluster center, the potential of each point is adjusted using Equation (5).

$$P_i = p_i - p_k e^{-\beta\|x_i - x_k\|^2} \quad (5)$$

In this equation, x_k denotes the center of the k-th cluster, and p_k represents its potential. The algorithm continues until a suitable number of cluster centers is found. When the cluster estimation method is applied to a set of input and output data, each cluster center represents the system's behavioral characteristics. Therefore, each cluster center can serve as the basis for a rule defining the system's behavior.

3.2. ANFIS Network Structure

The mentioned ANFIS network has the limitation of piecewise differentiability, and structurally, its only constraint is being feedforward. For simplicity, let's consider a feedforward neural network with two inputs, x and y, and one output, z Each input has two rules of the TSK type:

Rule 1: If x is A1 and y is B1, then f1= p1x + q1y + r1 (6)

Rule 2: If x is A2 and y is B2, then f2= p2x + q2y + r2 (7)

The TSK fuzzy inference network and its corresponding neuro-fuzzy structure are depicted in Figure (2), which will be elucidated in detail later [4].

Layer One: Each node in this layer is a square node, with a function expressed as follows:

$$O_i^1 = \mu_{Ai}(x) \quad (8)$$

In this Equation, x is the input data to node i, and Ai is the linguistic label associated with this node's function. Typically, $\mu_{Ai}(x)$ is bell-shaped or Gaussian, with maximum and minimum values of one and zero, respectively.

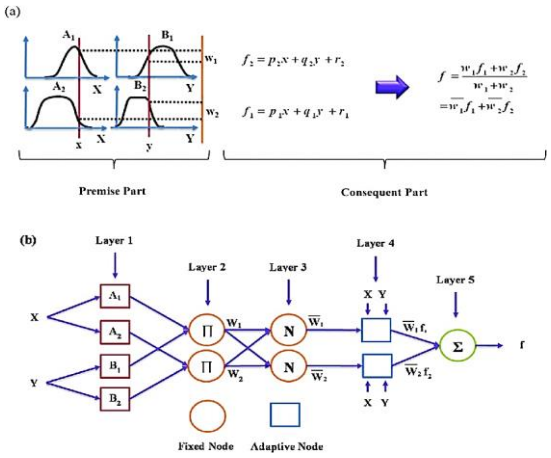

Figure 2. a) TSK fuzzy inference system, b) ANFIS network equivalent to the system [30].

For the bell-shaped function:

$$\mu_{Ai}(x) = \frac{1}{1+\left[\left(\frac{x-c_i}{a_i}\right)^2\right]^{b_i}} \quad (9)$$

For the Gaussian function:

$$\mu_{Ai}(x) = exp\left\{-\left(\frac{x-c_i}{a_i}\right)^2\right\} \quad (10)$$

Various forms of membership functions can be employed in the linguistic label Ai. In fact, any continuous and differentiable function, such as triangular and trapezoidal functions, is suitable for use as a node function. It's important to note that the parameters of this layer are regarded as premise parameters.

Layer Two: Each node in this layer is circular, denoted by $\prod$ in the diagram. Nodes in this layer receive input signals and transmit the output to the next layer. The output of each node in this layer represents the strength of the rule. Essentially, any operator capable of performing the AND operation can be used in this layer.

$$\omega_i = \mu_{Ai}(x) * \mu_{Bi}(x), \quad i = 1,2 \quad (11)$$

Layer Three: Each node in this layer is circular, denoted by N in the diagram. The ith node in this layer calculates the ratio of the strength of the ith rule to the sum of the strengths of all rules. For convenience, the outputs of this layer are called normalized weights.

$$\overline{\omega_l} = \frac{\omega_i}{\omega_1+\omega_2}, \quad i = 1,2 \quad (12)$$

Layer Four: Nodes of this layer are square, and its function is as follows:

$$O_i^4 = \overline{\omega_i} f_i = \overline{\omega_i}(p_i x + q_i y + r_i) \quad (13)$$

Where $\overline{\omega_l}$ is the output of the third layer, and $\{p_i, q_i, r_i\}$ are sets of parameters. The parameters of this layer are known as consequent parameters.

Layer Five: The only node in this layer is circular, denoted by $\sum$, and the overall output is calculated based on Equation (14).

$$O_i^5 = overall\ output = \sum \overline{\omega_l} f_i = \frac{\sum \overline{\omega_i} f_i}{\omega_i} \quad (14)$$

Given the TSK fuzzy inference system, based on the values given as premise parameters, the overall output can be expressed as a linear combination of the consequent parameters.

$$f = \frac{w_1}{w_1+w_2} f_1 + \frac{w_2}{w_1+w_2} f_2 = \overline{\omega_1} f_1 + \overline{\omega_2} f_2$$

$$= (\overline{\omega_1} x_1) p_1 + (\overline{\omega_1} y_1) q_1 + (\overline{\omega_1} r_1) + (\overline{\omega_2} x_2) p_2 + (\overline{\omega_2} y_2) q_2 + (\overline{\omega_2} r_2) \quad (15)$$

In the framework of the system's dynamics, during the forward

propagation phase, operational signal transitioning from the input layer (Layer One) to the fourth layer. Within this phase, the consequent parameters are estimated utilizing the least squares error methodology. Conversely, in the backward propagation phase, the error gradient is computed in a reverse direction, facilitating the update of the premise parameters through the application of the gradient descent algorithm. The key parameters involved in this process are systematically summarized in Table (2).

Table 2. ANFIS algorithm steps [30].

Component	Forward Movement	Backward Movement
Preceding parameters	constant	Gradient descent algorithms
Tally parameters	least squares	constant
signals	Output nodes	Error rates

4. Data Collection and Interpretation

The primary goal of employing intelligent networks is to offer a model for data that cannot be defined by a specific function. Therefore, in this section, the implementation of the ANFIS algorithm requires sufficient and categorized data that represent and illustrate the characteristics and features of the study's subject so that they can undergo training (learning). Network training necessitates two sets of data: input data and output data. In the current study, two scenarios labeled ANFIS1 and ANFIS2 have been developed and examined to calculate stability and safety factors for circular failure. The steps involved in working with adaptive neuro-fuzzy networks are depicted in Figure (3).

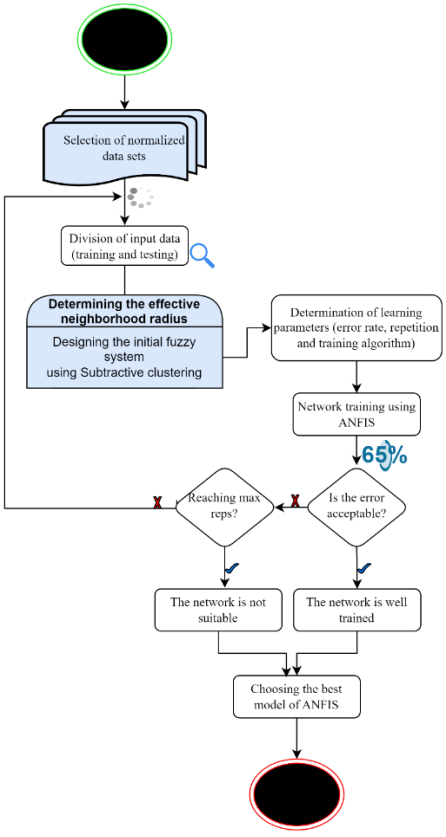

Figure 3. Process steps of adaptive neural-fuzzy inference network [38].

4.1. Simulation of Circular Failure

In this section, for implementing the adaptive neuro-fuzzy network, six input data parameters are considered: unit weight (γ), cohesion (C), internal friction angle (φ), geometric parameters of the slope including slope height (H), slope angle (β), and external forces comprising the pore water pressure ratio (r_u). Additionally, two output datasets are included: the safety factor for the first scenario (ANFIS1) and the stability condition for the second scenario (ANFIS2). For constructing the network aimed at predicting circular failure, a dataset comprising 103 data points gathered from diverse studies by Manouchehrian et al. has been utilized. A subset of these data points is illustrated in Table (3) to provide readers with concrete examples [37].

Table 3. Data used to build the ANFIS model in predicting circular failure.

Number	Stability	SF	r_u	H(m)	β(°)	φ(°)	c(kpa)	γ(KN/m³)
1	IS	1.11	0	8.23	35	15	26.34	8.68
2	IS	1	0	3.66	30	0	11.49	16.5
3	S	1.88	0	30.5	20	25	14.36	18.84
4	S	1.78	0	100	35	35	29.42	28.44
5	S	1.99	0	100	35	38	39.23	28.44
6	IS	1.25	0	40	30	27	16.28	20.6
7	IS	1.13	0	50	20	17	0	14.8
8	IS	1.02	0	88	30	26	11.97	14
9	IS	1.09	0	6	30	0	25	18.5
10	IS	0.78	0	6	30	0	12	18.5

Stability (S), Instability (IS)

Following this, the correlation coefficients between paired data and the statistical properties pertaining to the 103 analyzed data points are comprehensively outlined in Tables (4 and 5).

Table 4. Statistical characteristics used to build the model.

Parameter	γ(KN/m³)	c(kpa)	φ(°)	β(°)	H(m)	r_u	SF
Min	12	0	0	16	3.6	0	0.63
Max	28.44	50	45	53	214	0.5	2.31
Average	19.96	10.48	26.63	33.26	40.73	0.21	1.28
Median	19.98	8.33	30	30.5	25.75	0.25	1.19
Standard Deviation	3.54	10.8	10.8	9.5	42.96	0.18	0.4
Variance	12.53	116.73	116.57	90.23	1845.94	0.03	0.16

Table 5. Pairwise correlation coefficient matrix of model input parameters.

	γ(KN/m³)	c(kpa)	φ(°)	β(°)	H(m)	r_u	SF
γ(KN/m³)	1	0.42	0.34	0.14	0.47	-0.01	0.26
c(kpa)		1	0.06	0.21	0.31	-0.19	0.18
φ(°)			1	0.53	0.21	0.08	0.32
β(°)				1	0.11	-0.1	-0.2
H(m)					1	-0.16	-0.17
r_u						1	-0.21
SF							1

In this phase, two distinct ANFIS networks, referred to as ANFIS1 and ANFIS2, were developed to estimate the safety factor and assess stability conditions, assisting in categorizing slopes as stable or unstable. Input data for these networks is normalized to a range of zero to one. Key parameters in adaptive neuro-fuzzy networks include the type and quantity of membership functions, as well as the number of rules applied. The Subtractive Clustering Method algorithm was employed in this research to determine these parameters. Thus, the variable parameter in this network is the influence range of each membership function, defined by the radii parameter in the SCM algorithm. The network's stopping criterion is set to achieve either zero error or complete 500 iterations. Overtraining, a potential issue during extensive network training, can be prevented by monitoring the trend of Mean Squared Error (MSE) changes in the test data. Thus, identifying the saturation point occurs when the training data error decreases while the test data MSE begins to increase. In both models (Safety Factor and Stability State), determining the optimal network involved incrementally increasing the influence range of the membership function from 0.2 to 0.5 in steps of 0.05. The algorithm was iterated on ten randomly selected data sets during each step of expanding the range. The outcomes at each increment were assessed based on various metrics, including regression analysis, training MSE, test MSE, training RMSE, and test RMSE, detailed in Tables 6 and 7. Based on the comparison, an influence range of 0.2 was selected as the optimal range for the models.

4.1.1. Training of the ANFIS Network for Determining the Safety Factor and Its Results

The inputs of the network comprise the geotechnical parameters of the slope-forming materials and the geometric characteristics of the slope, while its output is the safety factor. During the training of ANFIS1 network, both input and output data (safety factor) were fed into the system for modeling. The network structure for the input parameters is outlined in Table (8) and illustrated in Figure (4).

At first, the network's training was scheduled for 500 iterations, but analysis of the test data error trend, depicted in Figure (4), indicated that stability was achieved after 384 iterations. No significant changes in the test data error were observed beyond this point. Hence, 384 iterations were identified as the optimal training period.

Table (9) presents the desired and predicted outputs for the test dataset, while Figure (5) displays the simulation results based on the correlation coefficient between the desired outputs and the outputs of the ANFIS1 network. In Figure (5), R is used to denote the correlation coefficient between the actual and predicted results of the network for both training and testing datasets (where Y represents the predicted values and T indicates the actual values). The outcomes reveal that the correlation coefficient for both data groups is nearly 1, indicating the effective performance of the network.

Also, In Figures (6 and 7), the network's predicted values for the training and test datasets are compared with the desired network outputs. As depicted in Figure (6), the mean error for the training data is close to zero, and the standard deviation of the measured errors is 0.005, indicating the network's outstanding performance for the training data. Furthermore, as shown in Figure (7), the network's Mean Squared Error for the test data is 0.025, with an average error of 0.05 and a standard deviation of the measured errors at 0.1, highlighting the network's strong generalization capability.

In Table (9), among the 19 tested data points, it is evident that data number 18 exhibits the greatest disparity in terms of safety factor, marking it as the most critical point in the mine wall. The error in data number 18 amounts to 35%, a discrepancy clearly visible in Figure 7.

Table 6. Results from ANFIS for different influence ranges to determine safety factor.

Test correlation coefficient	The square of the sum of squares of the test error	The sum of squares of the test error	Correlation coefficient of education	The square of the sum of squares of the training error	sum of squares of training error	influence range
0.938	0.15	0.025	1	0.005	$^{5-}$e* 2.61	0.2
0.907	0.17	0.032	1	0.005	$^{5-}$e* 2.61	0.25
0.72	0.32	0.1	1	0.005	$^{5-}$e* 2.61	0.30
0.76	0.29	0.083	1	0.005	$^{5-}$e* 2.61	0.35
0.81	0.25	0.063	1	0.005	$^{5-}$e* 2.61	0.40
0.84	0.23	0.054	1	0.005	$^{5-}$e* 2.61	0.45
0.77	0.29	0.089	1	0.005	$^{5-}$e* 2.61	0.50

Table 7. Results from ANFIS for different influence ranges to determine the stability state.

Test correlation coefficient	The square of the sum of squares of the test error	The sum of squares of the test error	Correlation coefficient of education	The square of the sum of squares of the training error	sum of squares of training error	influence range
0.987	0.08	0.006	1	4.8* e^{-7}	2.35* e^{-13}	0.2
0.91	0.21	0.045	1	8.23* e^{-7}	2.35* e^{-13}	0.25
0.96	0.14	0.021	1	7.18* e^{-7}	2.35* e^{-13}	0.3
0.97	0.11	0.014	1	1.00* e^{-6}	1.01* e^{-12}	0.35
0.93	0.19	0.034	1	4.6* e^{-6}	2.13* e^{-11}	0.4
0.88	0.23	0.054	1	1.36* e^{-6}	1.86* e^{-12}	0.45
0.86	0.26	0.069	1	1.82* e^{-5}	3.31* e^{-12}	0.50

Table 8. Specifications and structure of ANFIS1 network.

1143	Number of nodes
567	Number of linear parameters
972	Number of nonlinear parameters
1539	Total number of parameters
84	Number of training data
19	Number of test data
81	Number of fuzzy rules
384	Number of courses (Epoch)

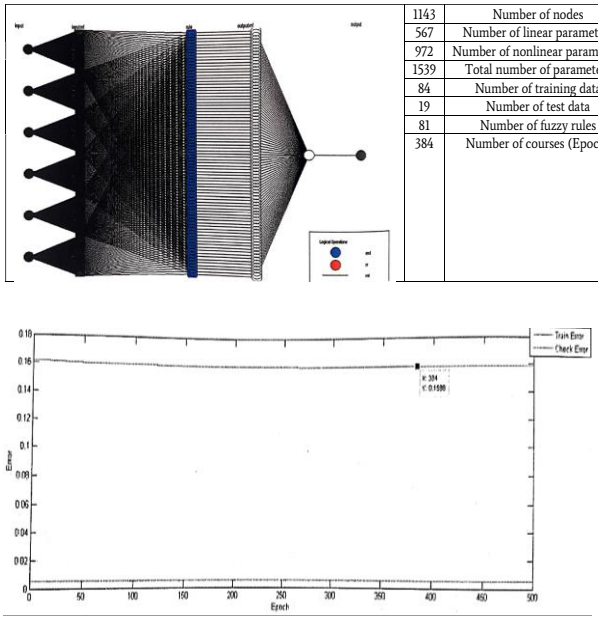

Figure 4. Error changes of training and testing data during 500 training periods related to ANFIS1 network.

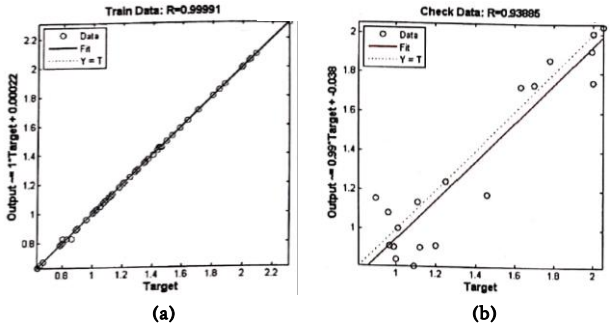

(a) (b)

Figure 5. Correlation coefficient of actual values and output of ANFIS1 for a) training and b) test data.

4.1.2. Training of the ANFIS Network for Determining Stability State and Its Results

The input parameters for this network include the geotechnical properties of the slope-forming materials and the geometric characteristics of the slope. The network yields a value of zero to denote a failure state and one to indicate stability. Information regarding the chosen optimal network configuration, along with the network structure pertaining to the input parameters, is presented in Table (10) and depicted in Figure (9).

During this phase, the initial plan for the network involved 500

training iterations. However, upon analyzing the test data error trend illustrated in Figure (8), it became evident that the network stabilized after 300 iterations, with no notable changes in the test data error thereafter. As a result, 300 iterations were identified as the optimal training period.

Table (11) provides the desired and predicted outputs for the test dataset, and Figure (9) depicts the simulation results based on the correlation coefficient between the desired outputs and the outputs of the ANFIS2 network. In this figure, R is employed as the correlation coefficient between the actual results and the network's predictions for both the training and test data (where Y denotes the predicted value, and T signifies the desired value). As per the findings, the correlation coefficient for both the training and test data is close to 1, indicating a strong performance by the network.

Table 9. The output of the ANFIS1 network related to the test data set.

Number	Predicted outputs	Desired outputs
1	0.92	0.97
2	0.91	0.99
3	0.92	1.2
4	0.85	1
5	1.16	0.9
6	2.04	2.05
7	1.75	2
8	1.01	1.01
9	1.73	1.63
10	1.74	1.7
11	1.24	1.25
12	0.91	1.12
13	2	2
14	1.14	1.11
15	1.18	1.46
16	1.08	0.96
17	1.92	1.99
18	0.81	1.09
19	1.87	1.78

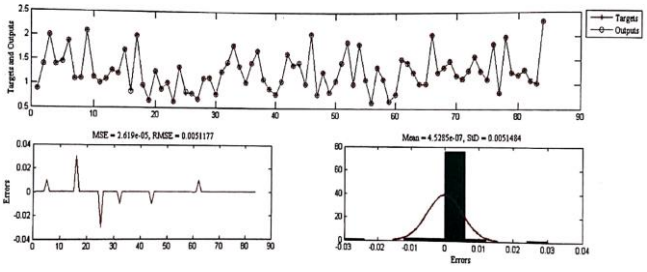

Figure 6. Results of ANFIS1 network for training data.

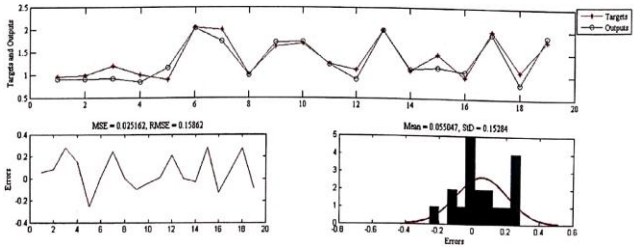

Figure 7. Results of ANFIS1 network for test data.

19 tested data in Table (11) clearly shows that data number 10 has the highest error in terms of stability and this point is identified as the most critical point in the mine wall.

In Figures (10 and 11), the network's predictions for both the training and test datasets are contrasted with their respective desired outputs. As depicted in Figure (10), both the mean error and the standard deviation of the measured errors for the training data are zero. This underscores the network's exceptional performance in handling the training data. Moreover, Figure (11) illustrates that the network's predictions were consistently accurate, with only a single data point exhibiting a slight deviation, where the prediction was close to but not exactly 1. The Mean Squared Error (MSE) of the network for the test data is computed to be 0.006, with an average error of 0.013 and a standard deviation for the measured errors at 0.08. Taken together, these metrics indicate a high generalization ability of the network.

Table 10. Specifications and structure of the ANFIS2 network.

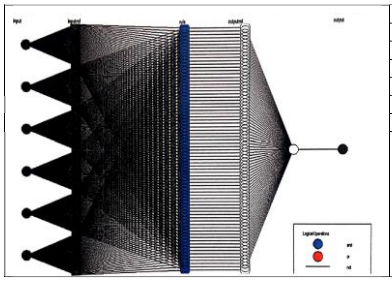

1059	Number of nodes
525	Number of linear parameters
900	Number of nonlinear parameters
1425	Total number of parameters
84	Number of training data
19	Number of test data
75	Number of fuzzy rules
300	Number of courses (Epoch)

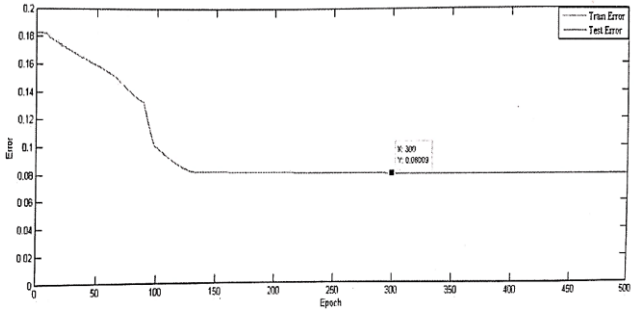

Figure 8. Error changes of training and testing data during 500 training periods related to ANFIS2 network.

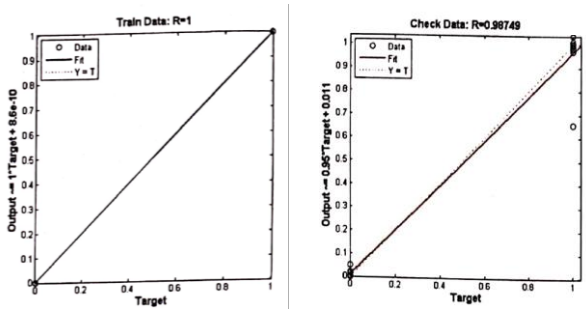

(a) (b)

Figure 9. Correlation coefficient of actual values and ANFIS2 output for a) training and b) test data.

Table 11. ANFIS2 network output related to the test data set.

Number	Predicted outputs	Desired outputs
1	0	0
2	0	0
3	1	1
4	1	1
5	1.04	1
6	0.02	0
7	0.02	0
8	0.99	1
9	0	0
10	0.66	1
11	1.01	1
12	0.98	1
13	1	1
14	1	1
15	0	0
16	0	0
17	0.05	0
18	0	0
19	0.97	1

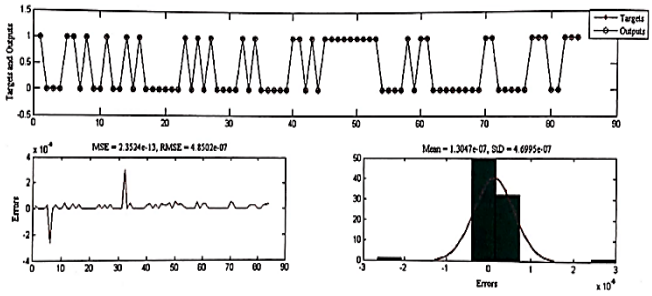

Figure 10. Results of ANFIS2 network for training data.

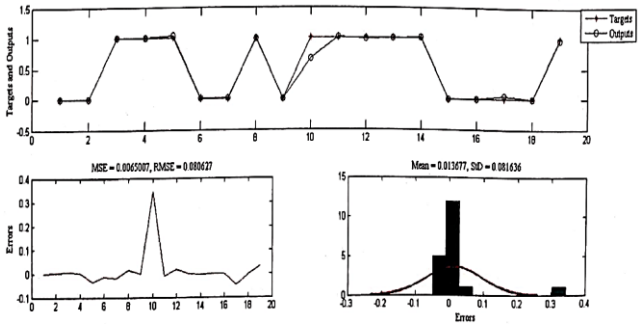

Figure 11. Results of ANFIS2 network for test data.

5. Conclusion

Determining the slope of pit walls is a critical aspect in open-pit mine design. Setting wall slopes too low leads to increased waste removal volume, while steeper slopes may compromise safety and raise collapse risks. Hence, selecting an optimal slope angle is vital to minimize waste excavation and reduce wall failure risks. In this study, two adaptive neuro-fuzzy inference networks were established to analyze slope static stability, focusing on estimating safety factors and stability conditions for circular failure scenarios. The models' inference systems follow the Sugeno methodology, with network parameters determined using the Subtractive Clustering Method. A dynamic learning algorithm was employed for effective network training. During the training process, 103 data points were used, with 80% for training and 20% for testing. Geotechnical parameters, slope geometry, and external forces were selected as inputs, including unit weight, cohesion, internal friction angle, slope angle, slope height, and pore water pressure ratio. Safety factor (ANFIS1) or stability state (ANFIS2) served as outputs. Metrics such as Mean Squared Error (MSE), Root Mean Squared Error (RMSE), and Correlation Coefficient (R) were utilized for evaluation. The ANFIS1 model exhibited MSE, RMSE, and R values of (2.61e-5, 0.005, and 1) for training data and (0.025, 0.15, and 0.938) for test data. For ANFIS2, these values were (2.35e-13, 4.8e-7, and 1) for training and (0.006, 0.08, and 0.987) for test data. The low error and high correlation coefficients demonstrate the networks' strong generalization capability, indicating their effectiveness in mapping relationships influencing slope stability analysis.

REFERENCES

[1] Duncan, J. M., & Wrigth, S. G. (2005). Soil strength and slope stability, John Willey & Sons. *Inc., Hoboken, New Jersey*, *297*.

[2]. Chen, C. H., Ke, C. C., & Wang, C. L. (2009). A back-propagation network for the assessment of susceptibility to rock slope failure in the eastern portion of the Southern Cross-Island Highway in Taiwan. *Environmental geology*, *57*, 723-733.

[3]. Chen, H., & Zeng, Z. (2013). Deformation prediction of landslide based on improved back-propagation neural network. *Cognitive computation*, *5*, 56-62.

[4]. Sah, N. K., Sheorey, P. R., & Upadhyaya, L. N. (1994, February). Maximum likelihood estimation of slope stability. In *International journal of rock mechanics and mining sciences & geomechanics abstracts* (Vol. 31, No. 1, pp. 47-53). Pergamon.

[5]. Goh, A. T. (1999). Genetic algorithm search for critical slip surface in multiple-wedge stability analysis. *Canadian geotechnical journal*, *36*(2), 382-391.

[6]. Goh, A. T. (2000). Search for critical slip circle using genetic algorithms. *Civil Engineering Systems*, *17*(3), 181-211.

[7]. McCombie, P., & Wilkinson, P. (2002). The use of the simple genetic algorithm in finding the critical factor of safety in slope stability analysis. *Computers and Geotechnics*, *29*(8), 699-714.

[8]. Lu, P., & Rosenbaum, M. S. (2003). Artificial neural networks and grey systems for the prediction of slope stability. *Natural Hazards*, *30*, 383-398.

[9]. Yang, C. X., Tham, L. G., Feng, X. T., Wang, Y. J., & Lee, P. K. K. (2004). Two-stepped evolutionary algorithm and its application to stability analysis of slopes. *Journal of computing in civil engineering*, *18*(2), 145-153.

[10]. Sakellariou, M. G., & Ferentinou, M. D. (2005). A study of slope stability prediction using neural networks. *Geotechnical & Geological Engineering*, *23*, 419-445.

[11]. Ferentinou, M. D., & Sakellariou, M. G. (2007). Computational intelligence tools for the prediction of slope performance. *Computers and Geotechnics*, *34*(5), 362-384.

[12]. Cheng, Y. M., Li, L., & Chi, S. C. (2007). Performance studies on six heuristic global optimization methods in the location of critical slip surface. *Computers and Geotechnics*, *34*(6), 462-484.

[13]. Park, H. J., Um, J. G., & Woo, I. (2008). The evaluation of failure probability for rock slope based on fuzzy set theory and Monte Carlo simulation. In *Proceedings of the 10th international symposium on landslides and engineered slopes* (pp. 1943-1949).

[14]. Li, L., Chi, S., Cheng, Y., & Lin, G. (2008). Improved genetic algorithm and its application to determination of critical slip surface with arbitrary shape in soil slope. *Frontiers of Architecture and Civil Engineering in China*, *2*, 145-150.

[15]. Choobbasti, A. J., Farrokhzad, F., & Barari, A. (2009). Prediction of slope stability using artificial neural network (case study: Noabad, Mazandaran, Iran). Arab J Geosci 2 (4): 311–319.

[16]. Zhou, K. P., & Chen, Z. Q. (2009, December). Stability prediction of tailing dam slope based on neural network pattern recognition. In *2009 Second international conference on environmental and computer science* (pp. 380-383). IEEE.

[17]. Shangguan, Z., Li, S., & Luan, M. (2009). Intelligent forecasting method for slope stability estimation by using probabilistic neural networks. *Electron J Geotech Eng Bundle*, *13*.

[18]. Ahangar-Asr, A., Faramarzi, A., & Javadi, A. A. (2010). A new approach for prediction of the stability of soil and rock slopes. *Engineering Computations*, *27*(7), 878-893.

[19]. Daftaribesheli, A., Ataei, M., & Sereshki, F. (2011). Assessment of rock slope stability using the Fuzzy Slope Mass Rating (FSMR) system. *Applied Soft Computing*, *11*(8), 4465-4473.

[20]. Chen, C., Xiao, Z., & Zhang, G. (2011). Stability assessment model for epimetamorphic rock slopes based on adaptive neuro-fuzzy inference system. *Electron J Geotech Eng*, *16*(A), 93-107.

[21]. Das, S. K., Biswal, R. K., Sivakugan, N., & Das, B. (2011). Classification of slopes and prediction of factor of safety using differential evolution neural networks. *Environmental Earth Sciences*, *64*, 201-210.

[22]. Park, H. J., Um, J. G., Woo, I., & Kim, J. W. (2012). Application of fuzzy set theory to evaluate the probability of failure in rock slopes. *Engineering Geology*, *125*, 92-101.

[23]. Erzin, Y., & Cetin, T. (2012). The use of neural networks for the prediction of the critical factor of safety of an artificial slope subjected to earthquake forces. *Scientia Iranica*, *19*(2), 188-194.

[24]. Kang, F., Li, J., & Ma, Z. (2013). An artificial bee colony algorithm for locating the critical slip surface in slope stability analysis. *Engineering Optimization*, *45*(2), 207-223.

[25]. Samui, P. (2013). Support vector classifier analysis of slope. *Geomatics, Natural Hazards and Risk*, *4*(1), 1-12.

[26]. Erzin, Y., & Cetin, T. (2013). The prediction of the critical factor of safety of homogeneous finite slopes using neural networks and multiple regressions. *Computers & Geosciences*, *51*, 305-313.

[27]. Manouchehrian, A., Gholamnejad, J., & Sharifzadeh, M. (2014). Development of a model for analysis of slope stability for circular mode failure using genetic algorithm. *Environmental Earth Sciences*, *71*, 1267-1277.

[28]. Liu, Z., Shao, J., Xu, W., Chen, H., & Zhang, Y. (2014). An extreme learning machine approach for slope stability evaluation and prediction. *Natural hazards*, *73*, 787-804.

[29]. Xue, X., & Xiao, M. (2017). Deformation evaluation on surrounding rocks of underground caverns based on PSO-LSSVM. *Tunnelling and Underground Space Technology*, *69*, 171-181.

[30]. Jang, J. S. (1993). ANFIS: adaptive-network-based fuzzy inference system. *IEEE transactions on systems, man, and cybernetics*, *23*(3), 665-685.

[31]. Kayadelen, C., Taşkıran, T., Günaydın, O., & Fener, M. (2009). Adaptive neuro-fuzzy modeling for the swelling potential of compacted soils. *Environmental Earth Sciences*, *59*, 109-115.

[32]. Echanobe, J., del Campo, I., & Bosque, G. (2008). An adaptive neuro-fuzzy system for efficient implementations. *Information Sciences*, *178*(9), 2150-2162.

[33]. Singh, R., Vishal, V., Singh, T. N., & Ranjith, P. G. (2013). A comparative study of generalized regression neural network approach and adaptive neuro-fuzzy inference systems for prediction of unconfined compressive strength of rocks. *Neural Computing and Applications*, *23*, 499-506.

[34]. Bashari, A., Beiki, M., & Talebinejad, A. (2011). Estimation of deformation modulus of rock masses by using fuzzy clustering-based modeling. *International Journal of Rock Mechanics and Mining Sciences*, *48*(8), 1224-1234.

[35]. Chiu, S. L. (1994). Fuzzy model identification based on cluster estimation. *Journal of Intelligent & fuzzy systems*, *2*(3), 267-278.

[36]. Guillaume, S. (2001). Designing fuzzy inference systems from data: An interpretability-oriented review. *IEEE Transactions on fuzzy systems*, *9*(3), 426-443.

[37]. Fattahi, H., Shojaee, S., Farsangi, M. A. E., & Mansouri, H. (2013). Hybrid Monte Carlo simulation and ANFIS-subtractive clustering method for reliability analysis of the excavation damaged zone in underground spaces. *Computers and Geotechnics*, *54*, 210-221.

[38]. Iranmanesh, Z., Khoshrou, S.H. (2015). Artificial Neural Networks Based on Fuzzy System and Fuzzy Neural Networks for Stability Assessment of Rock Slope in Choghart Iron Mine. *AmirKabir University of Technology, Tehran, Iran, February 2015*.